Supplement to "Global sensitivity analysis of a dam breaching model: To which extent is parameter sensitivity case-dependent?"

Flow chart of the numerical model

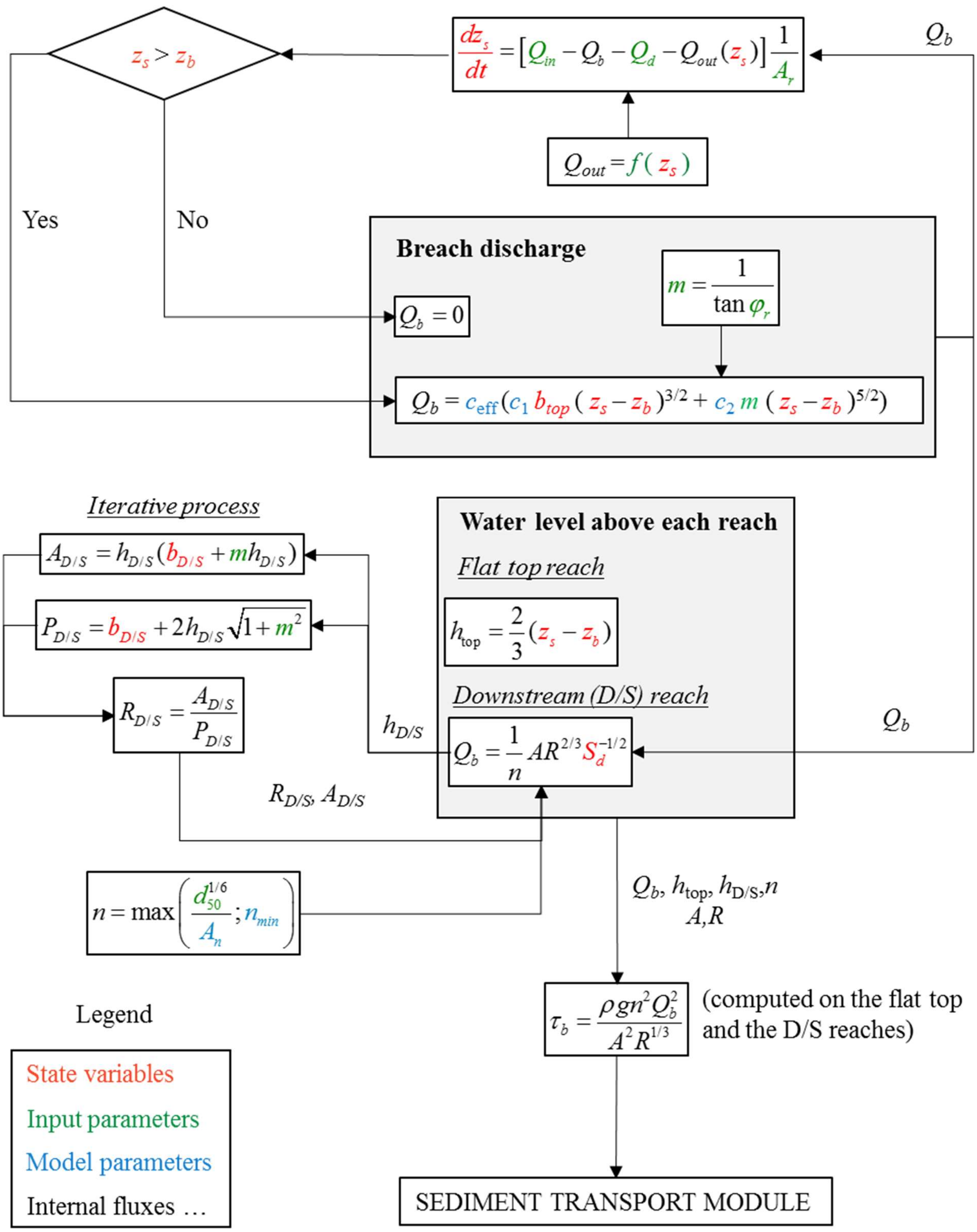

Figure S1 Flow chart of the hydrodynamic module of the implemented numerical model.

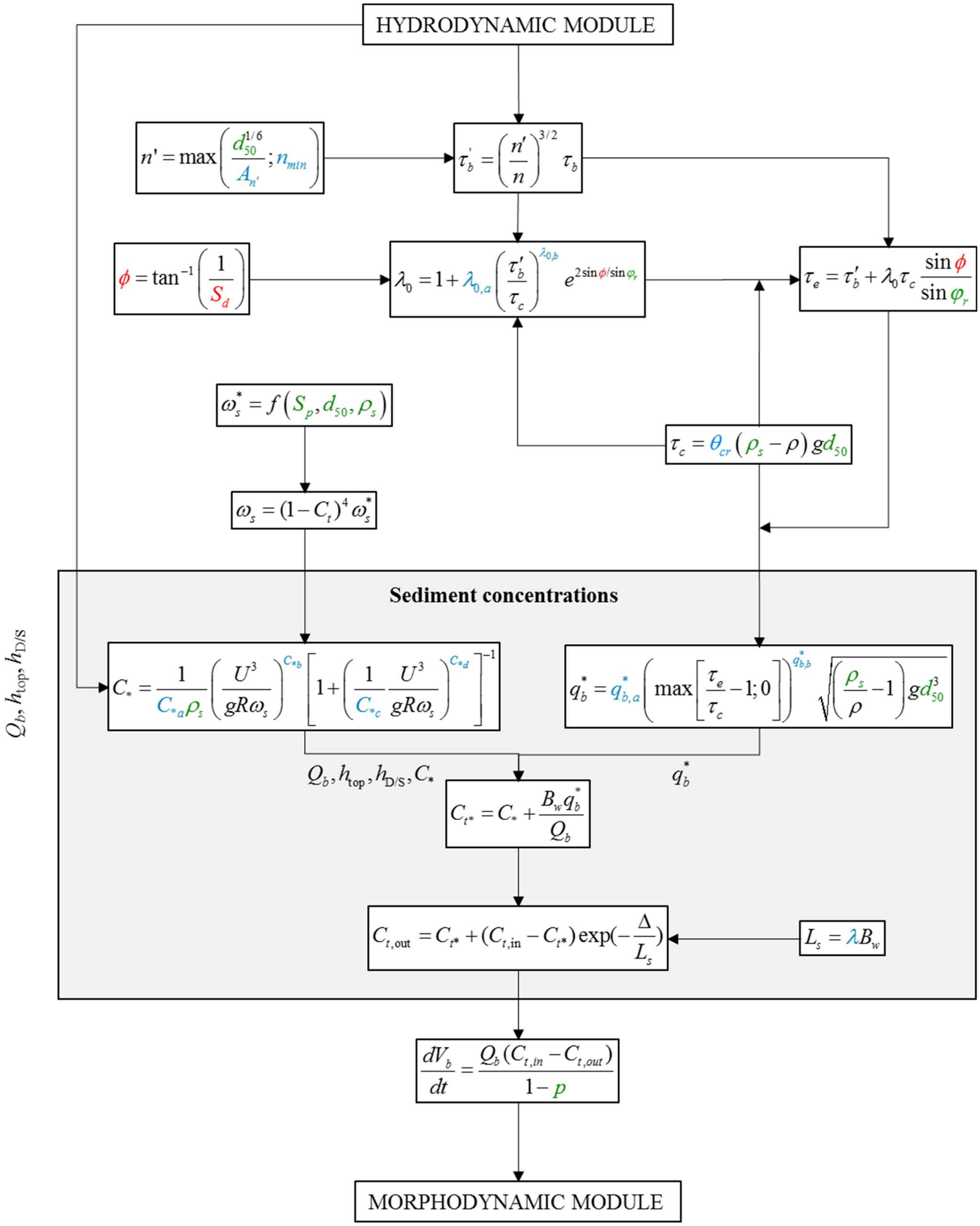

Figure S2 Flow chart of the sediment transport module.

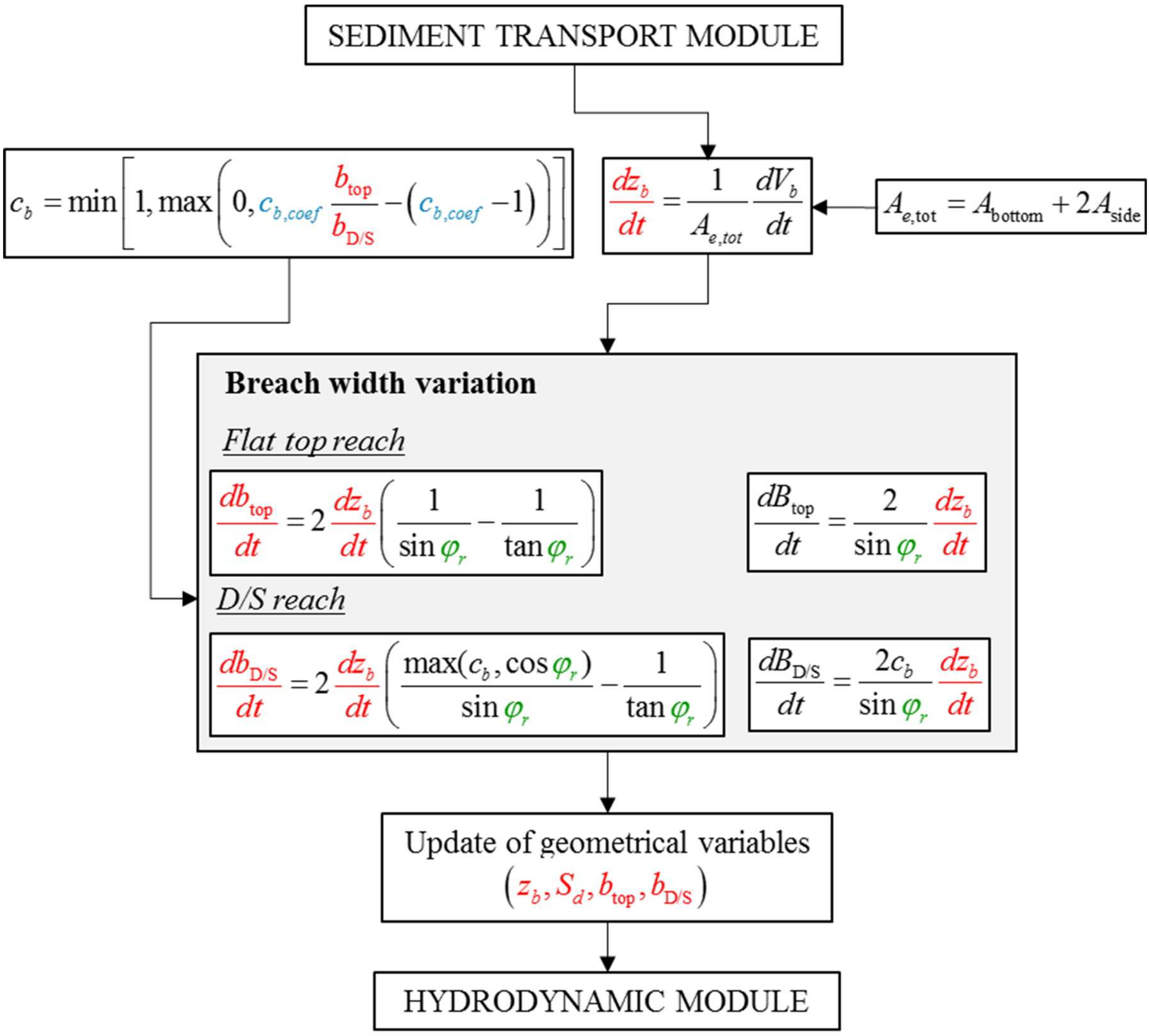

Figure S3 Flow chart of the morphodynamic module.

Table S1 Literature review (A).

Reference	Numerical model	Uncertainty analysis				
		Case study	Inputs type	PDF characterization	Sampling	Method/Indicator
Tsai et al. (2019)	Simplified physically based (0D)	1 field-scale dam	Independent (3 inputs)	Modeler expertise	PEM (7 runs)	Variance-based method Statistical moments of the outputs
Abdedou et al. (2020)	Detailed hydraulic model (1D) No dam model	1 field-scale dam	Independent (3 inputs)	Modeler expertise	Monte-Carlo (10^6) + 2 meta-models (10+100, each)	Confidence interval Outputs PDF
Froehlich and Goodell (2012)	1D hydraulic model 0D empirical breach model	1 field-scale dam	Independent (4 inputs)	Modeler expertise	PEM (16 runs)	Statistical moments of the outputs
Vorogushyn et al. (2011)	1D hydraulic model 0D probabilistic dike breach model 2D storage cell inundation model	1 field-scale fluvial dike case along a river (breaching possible at different places, simultaneously)	Dependent and independent (5 inputs)	MLE	Monte-Carlo (1000 runs)	Mean and percentiles Uncertainty bands
Kalinina et al. (2020)	1D hydraulic model No dam model	1 field-scale dam	Dependent (9 inputs)	MLE	Latin Hypercube (2000 runs of initial model to build meta-model + 10^6 runs of intermediate meta-model)	Sobol indices Outputs PDF
Pheulpin et al. (2020)	1D + 2D hydraulic models Fixed dam geometry	1 field-scale fluvial dike	Independent (3 inputs)	Modeler expertise	Monte-Carlo (200 runs of initial model to build each meta-model (2) + 5000 runs of each meta-model)	Sobol indices Outputs PDF
Goeury et al. (2022)	2D hydrodynamic model 0D breach model (Prescribed evolution)	1 field-scale river with multiple fluvial dikes	Independent (~300 inputs)	Modeler expertise	Monte-Carlo	PFI Delta indicator Outputs PDF

Notations and abbreviations: PEM = Point estimate method; MLE = Maximum likelihood estimation; PFI = Permutation feature importance.

Table S2 Literature review (B).

Reference	Numerical model	Uncertainty analysis				
		Case study	Inputs type	PDF characterization	Sampling	Method/Indicator
Froehlich (2008)	0D empirical breach model	1 field-scale dam	Independent (3 inputs)	MLE	Monte-Carlo (10^5 runs)	Mean and percentiles
Sattar (2014)	0D empirical breach model	General (field-scale dams)	Independent (6 inputs)	MLE	Monte-Carlo (250,000 runs)	MAD Percentiles Least square linearization technique
Ahmadisharaf et al. (2016)	4 different 0D empirical breach models	1 field-scale dam	Independent (3 inputs)	Modeler expertise	Latin Hypercube (10^4 for each model)	MAD Mean and percentiles Importance measure Coefficient of determination
Westoby et al. (2015)	2D hydrodynamic model 0D physically based breach model	1 field-scale dam	Independent (8 inputs)	Modeler expertise	Monte-Carlo (10^3 runs)	Uncertainty bands
Bellos et al. (2020)	1D hydrodynamic model 0D breach model (Prescribed evolution)	1 field-scale dam	Independent (7 inputs)	Modeler expertise	400 runs for MSM + Monte-Carlo (10^4 runs)	MSM Uncertainty bands Outputs PDF
Alhasan et al. (2016)	0D simplified physically based model	1 field-scale fluvial dike	Independent (9 inputs)	Modeler expertise	Latin Hypercube (5.10^6 runs)	MSM Uncertainty bands Outputs PDF
Peter et al. (2018)	Simplified physics-based dam breach model (0D)	1 field-scale dam	Independent (3 inputs)	Bayesian inference	Latin Hypercube (5.10^3)	Outputs PDF
Present study	Physically based (0D)	27 dams (lab + field scales)	Independent and dependent (21 inputs)	Modeler expertise	Monte-Carlo (4.10^3 / test)	Sobol indices Mean and percentiles

Notations and abbreviations: MSM = Morris screening method; MAD = Mean Absolute Deviation; B_{avg} = breach average width; MLE = maximum likelihood estimation.

Table S3 Frank's (2016) experimental parameters. L_r = reservoir length; l_r = reservoir width; A_r = reservoir area; h_d = dam height; L_k = dam crest length; $z_{b,ini}$ = initial notch depth; B_{ini} = initial notch width; d_{50} = median grain size; Q_{in} = inflow discharge; h_{cr} = critical flow depth.

	Test ID	L_r (m)	l_r (m)	A_r (m^2)	h_d (mm)	L_k (mm)	$z_{b,ini}$ (mm)	B_{ini} (mm)	d_{50} (mm)	Q_{in} (l/s)	h_{cr} (mm)
Scaling	11	0.61	0.5		150	50	50	200	0.86	2.62	14.1
	10	1.22	1		300	100	100	400	1.75	14.8	28.2
	8	2.44	2		600	200	200	800	3.78	83.6	56.3
	12	0.61	0.5		150	50	50	200	0.86	1.31	8.9
	13	1.22	1		300	100	100	400	1.75	7.4	17.7
	14	2.44	2		600	200	200	800	3.78	41.8	35.4
	15	0.61	0.5		150	50	50	200	0.43	2.62	14.1
	16	1.22	1		300	100	100	400	0.86	14.8	28.2
	17	2.44	2		600	200	200	800	1.75	83.6	56.3
Discharge	18									4.4	7.9
	19	3.44	2		300	100	100	400	1.75	8.8	12.5
	20									18.4	20.5
	21									35.2	31.6
Sediment	22								0.86		
	20	3.44	2		300	100	100	400	1.75	18.4	20.5
	23								3.78		
Initial breach width	20							400			
	24							500			
	25	3.44	2		300	100	100	600	1.75	18.4	20.5
	26							800			
	27							1200			
Crest length	28					0					
	20	3.44	2		300	100	100	400	1.75	18.4	20.5
	29					400					
Reservoir water surface area	40			6.88							
	36			26.88							
	41	3.44	2	33.02	300	100	20	80	1.75	0	0
	42			46.88							
	43			126.88							
	44			206.8							

Table S4 Characteristics of the independent variables considered in the present study. X_{ref} stands for the reference value of the related parameter.

	Symbol	Reference value	Variation range	α
Model parameters	c_{eff}	1	$\left[\frac{1.5}{1.7};\frac{2.2}{1.7}\right]$	2
	A_n	12 (field) 16 (lab)	[10; 20]	2
	$A_{n'}$	20	[18; 22]	5
	n_{min}	0.016	[0.01; 0.017]	3
	θ_{cr}	0.03	[0.025; 0.06]	3
	$\lambda_{0,a}$ $\lambda_{0,b}$	0.2 0.15	[0.15;0.25] [0.1;0.2]	3
	S_p	0.7	[0.2; 1]	4
	λ	3	[0.1; 4]	2
	$c_{b,coef}$	1.8	[1; 2.5]	2
Input parameters	S_u / S_d	2	[0.9; 1.1] X_{ref}	6
	L_k [m]	Test dependent	[-0.01; +0.01] + X_{ref}	6
	h_d [m]	Test dependent	[-0.01; +0.01] + X_{ref}	4
	φ_r	39.5	[38°; 41°]	4
	ρ_s [kg/m^3]	2600	[2400; 2800]	6
	d_{50} [mm]	Test dependent	[0.9; 1.1] X_{ref}	6
	p	0.44	[0.41; 0.47]	4
	Q_{in} [l/s]	Test dependent	[0.9; 1.1] X_{ref}	4

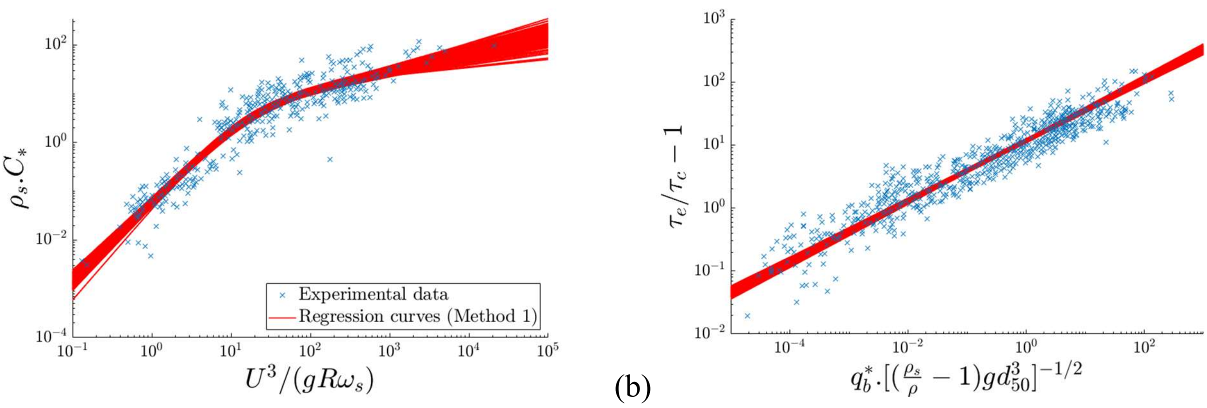

(a) (b)

Figure S4 Comparison between experimental data and regression curves based on (a) $\{C_a^*, C_b^*, C_c^*, C_d^*\}$ and (b) $\{q_{b,a}^*, q_{b,b}^*\}$ subsets generated using Method 1.

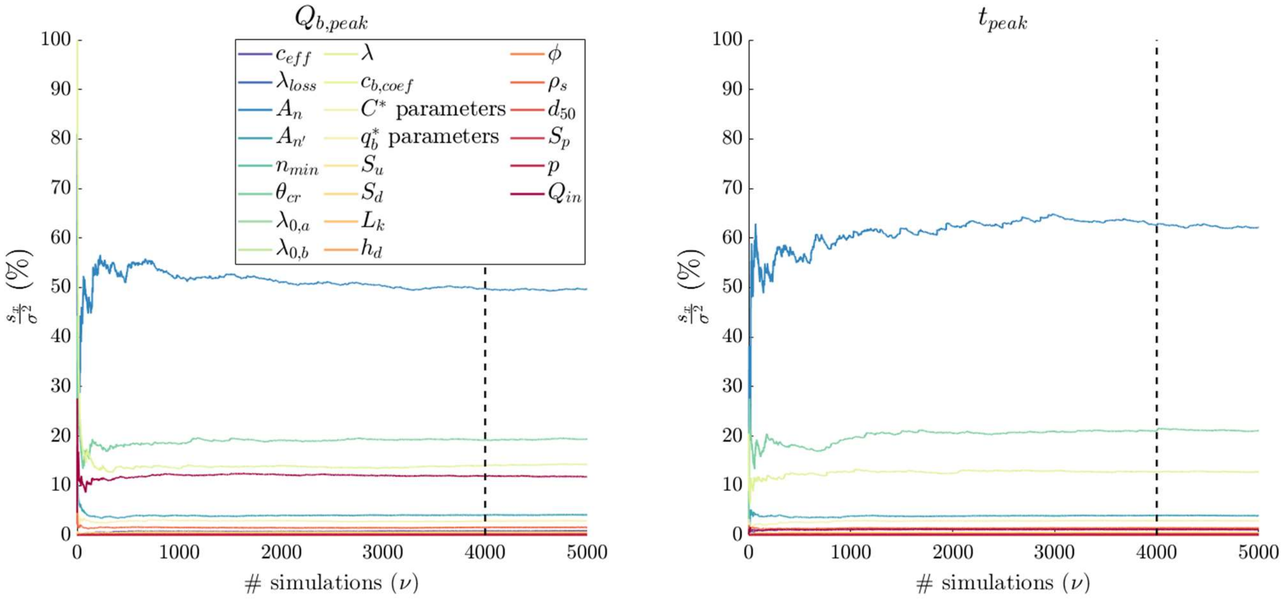

Figure S5 Convergence graphs of Sobol indices of total order for all input variables and both model outputs of interest using Method 1.

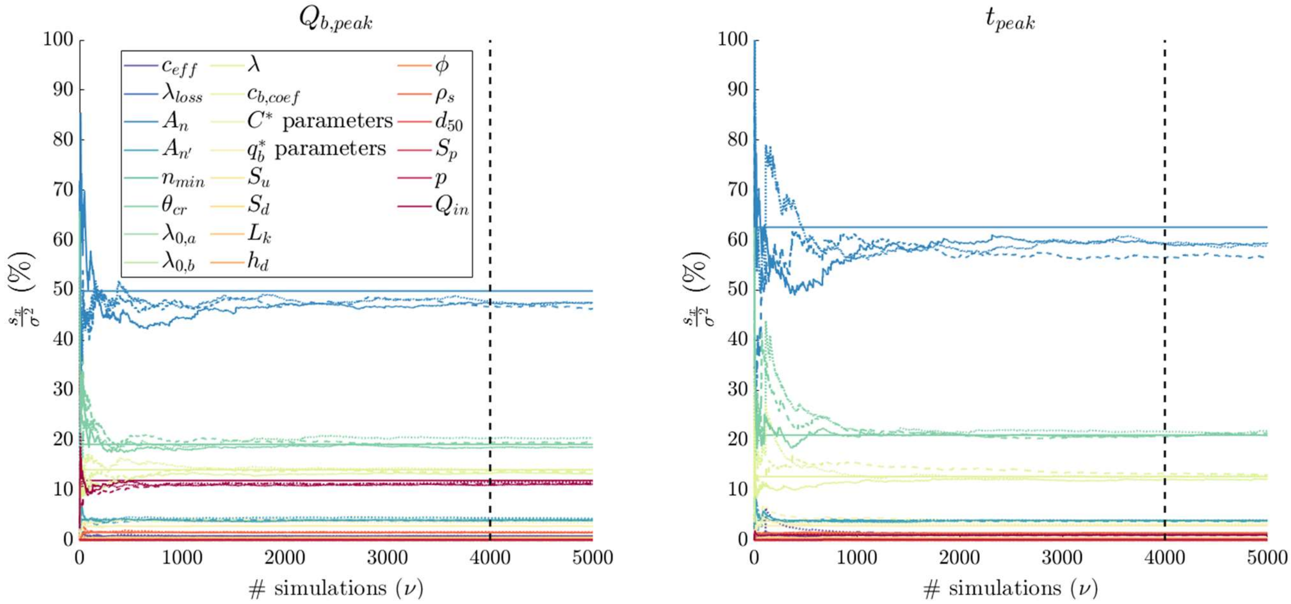

Figure S6 Accuracy and convergence evaluation of Sobol indices of total order obtained using Method 2. Legend: Horizontal plain lines = converged values obtained with Method 1; dashed curves = Method 2 with $k = 500$; dotted curves = Method 2 with $k = 1000$; plain curves = Method 2 with $k = 2000$.

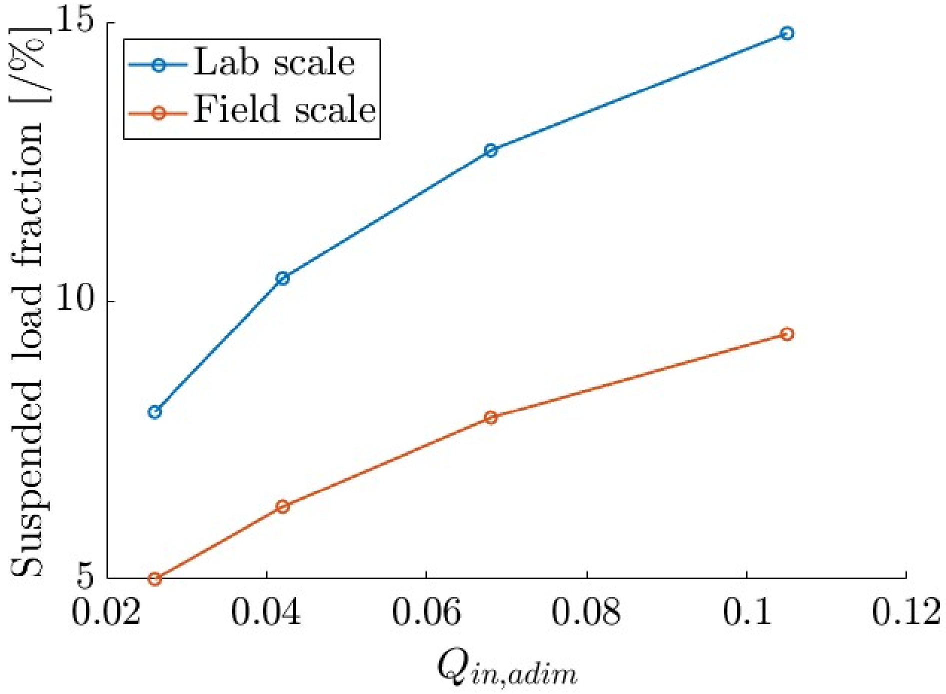

Figure S7 Mean percentage of overall sediment concentration corresponding to suspended load in lab and field -scale cases (Tests 18 to 21).

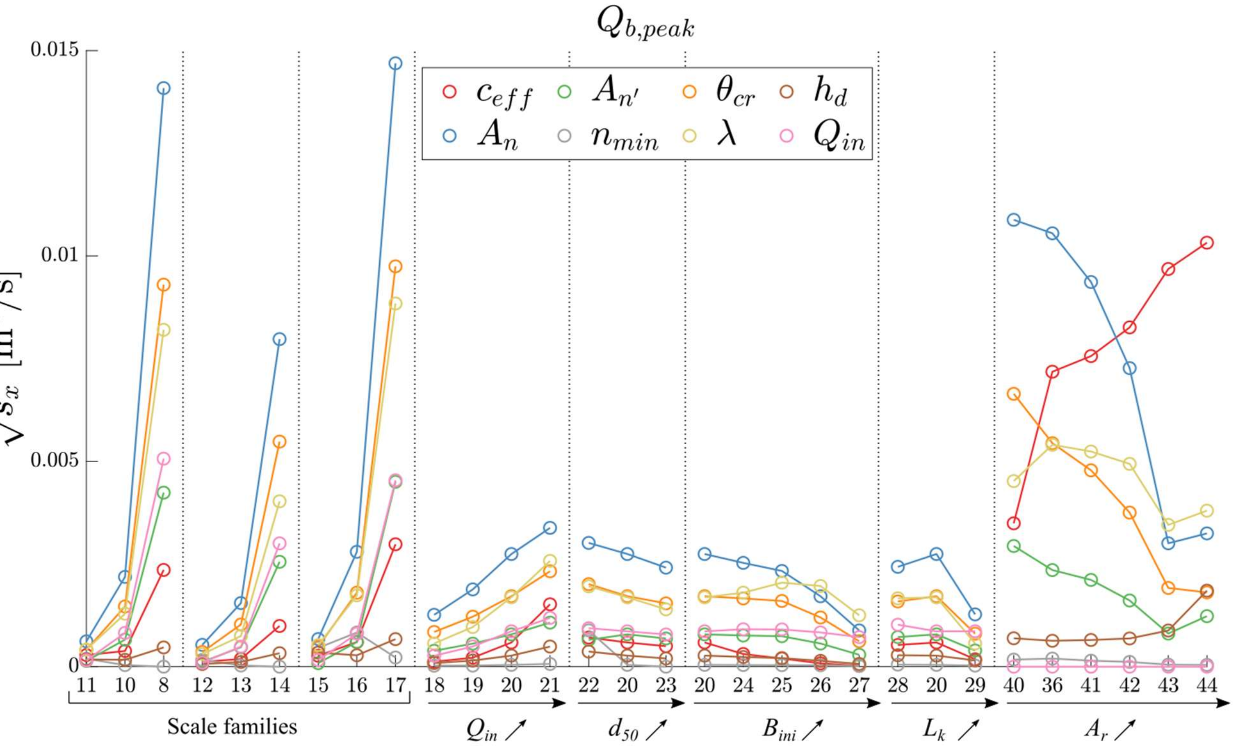

(a)

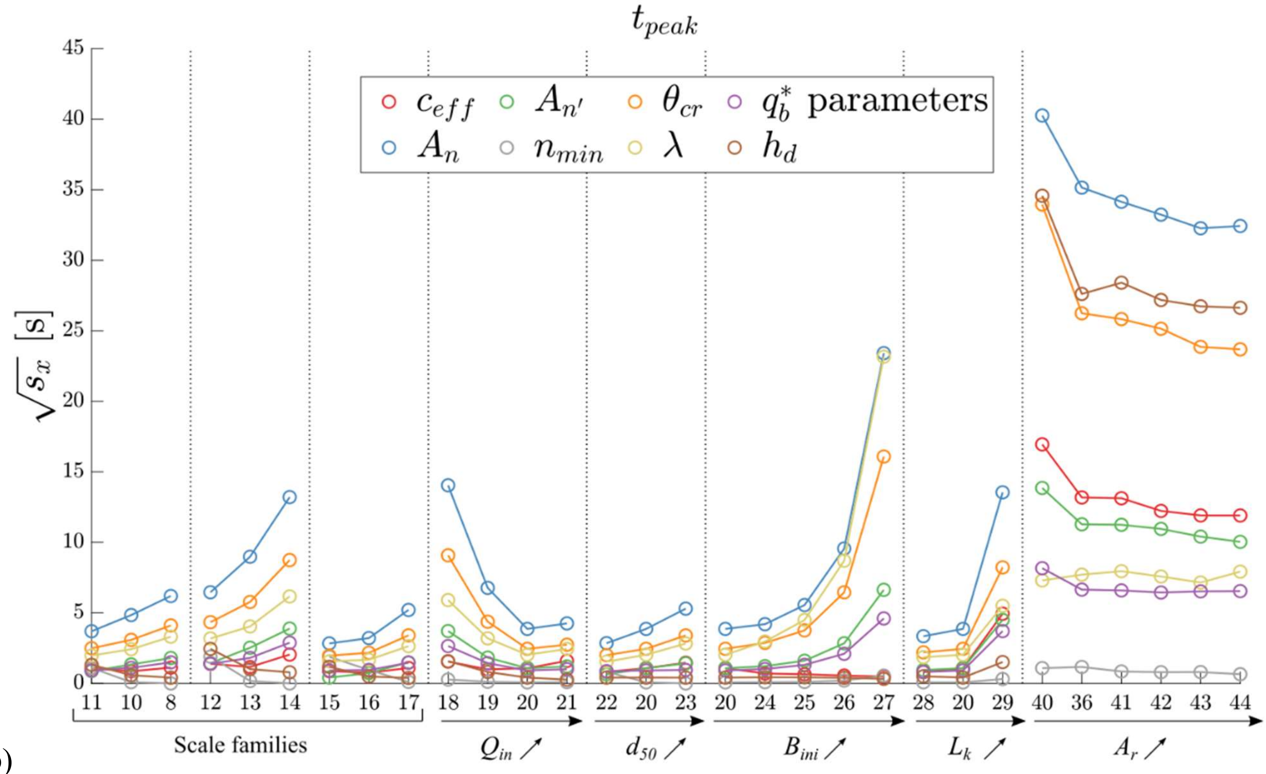

(b)

Figure S8 Significance descriptors in laboratory-scale configurations.

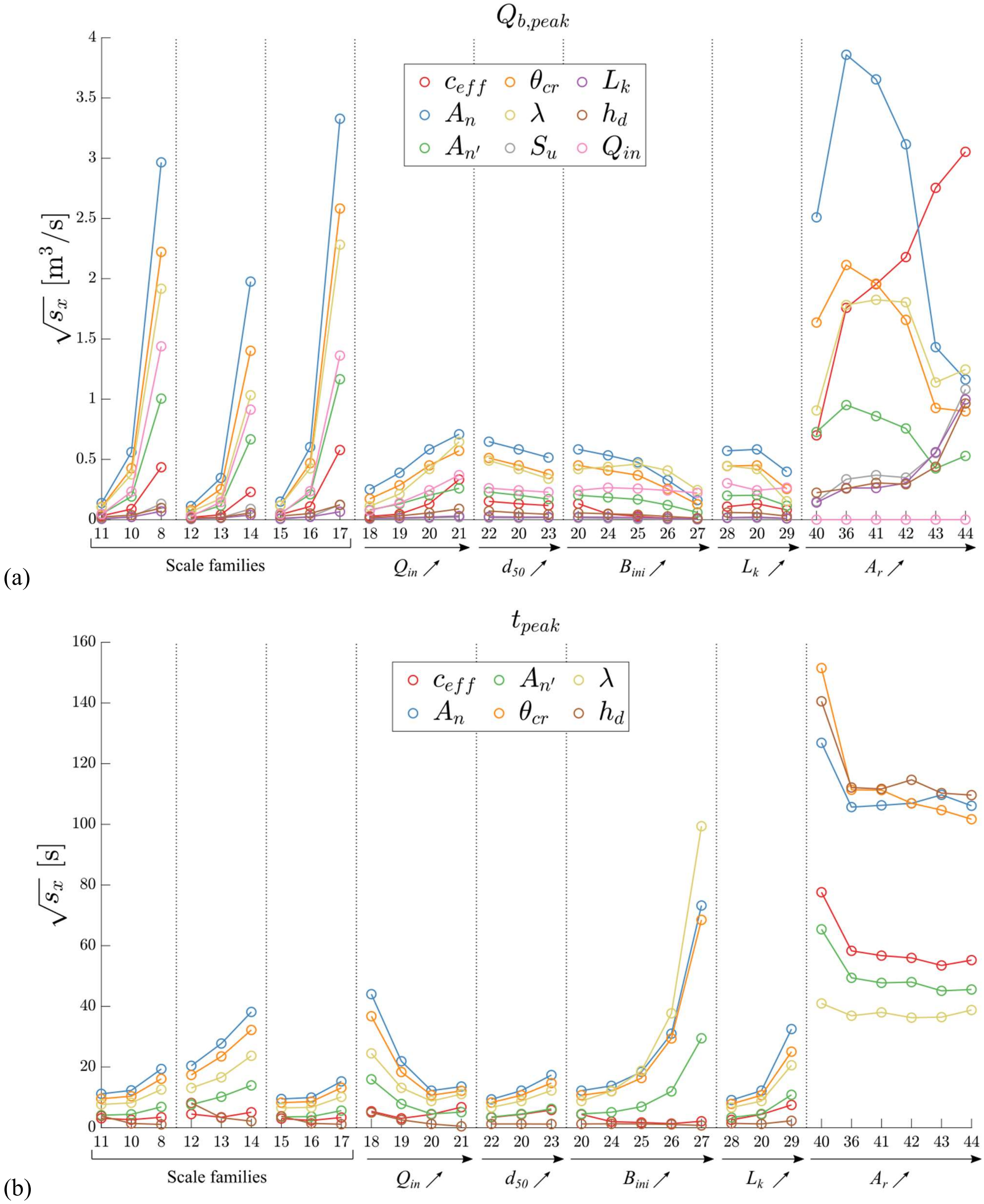

Figure S9 Significance descriptors in field-scale configurations.

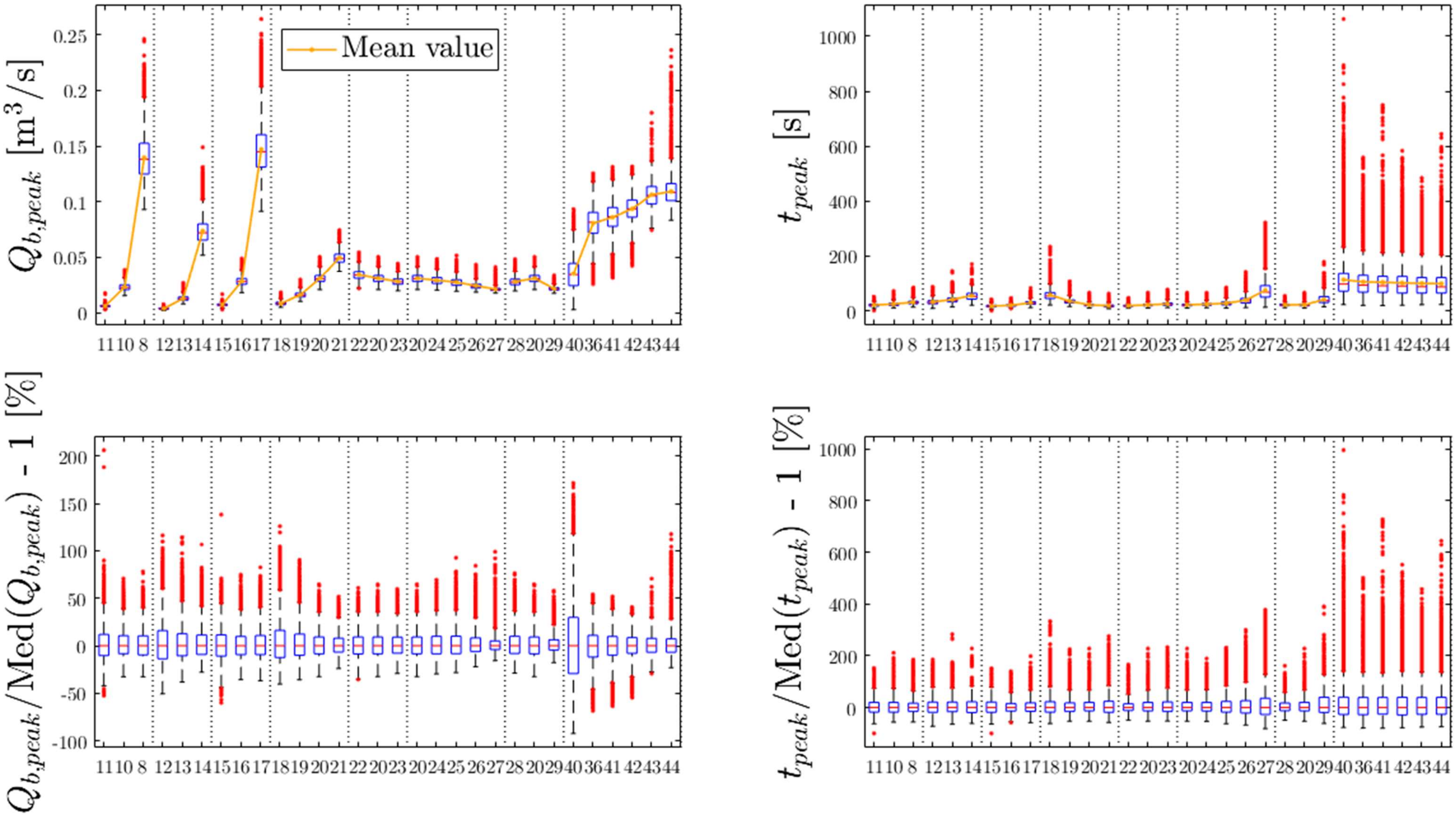

Figure S10 Boxplots of model outputs and their variation with respect to their median value in laboratory-scale configurations.

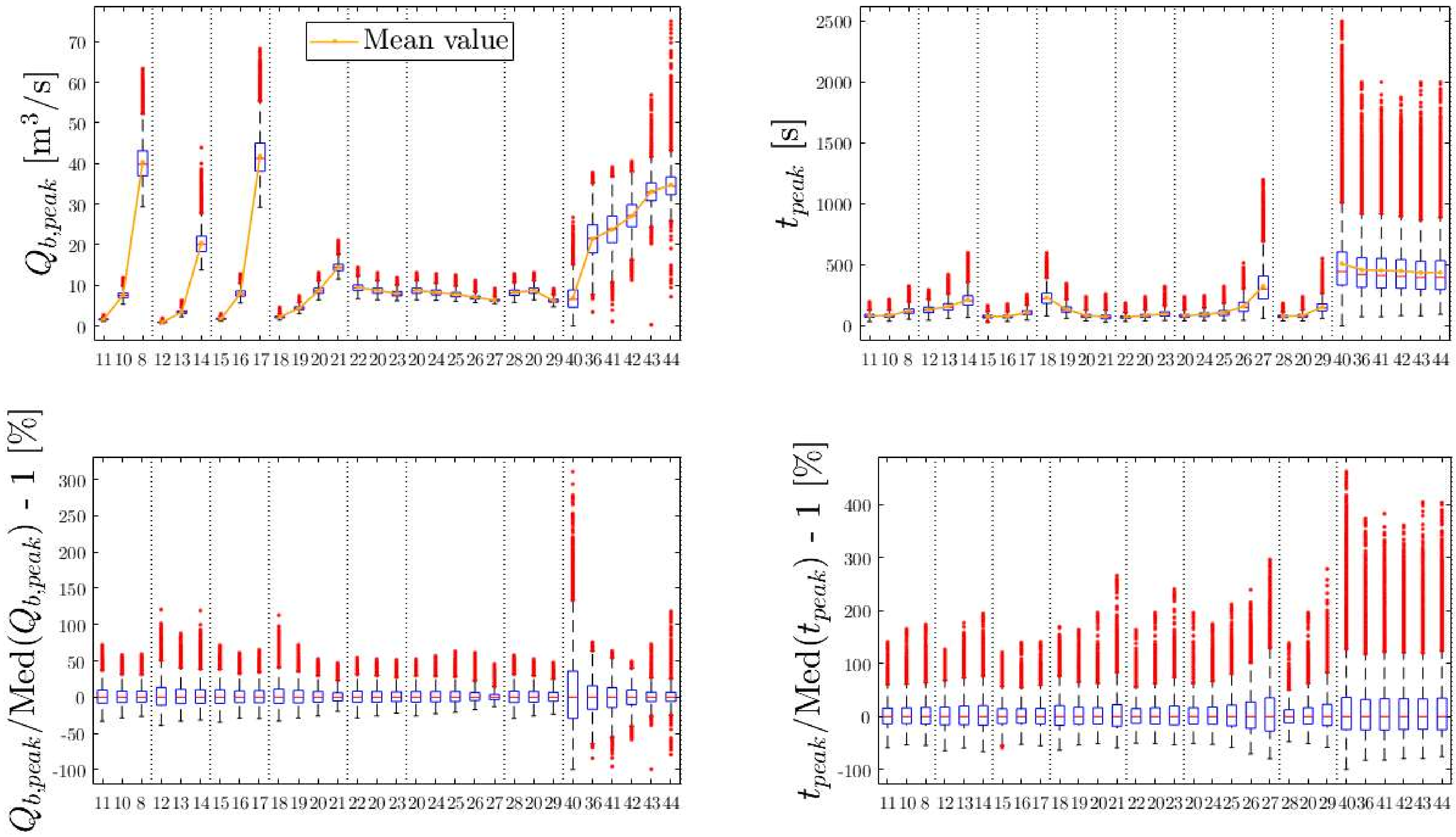

Figure S11 Boxplots of model outputs and their variation with respect to their median value in field-scale configurations.

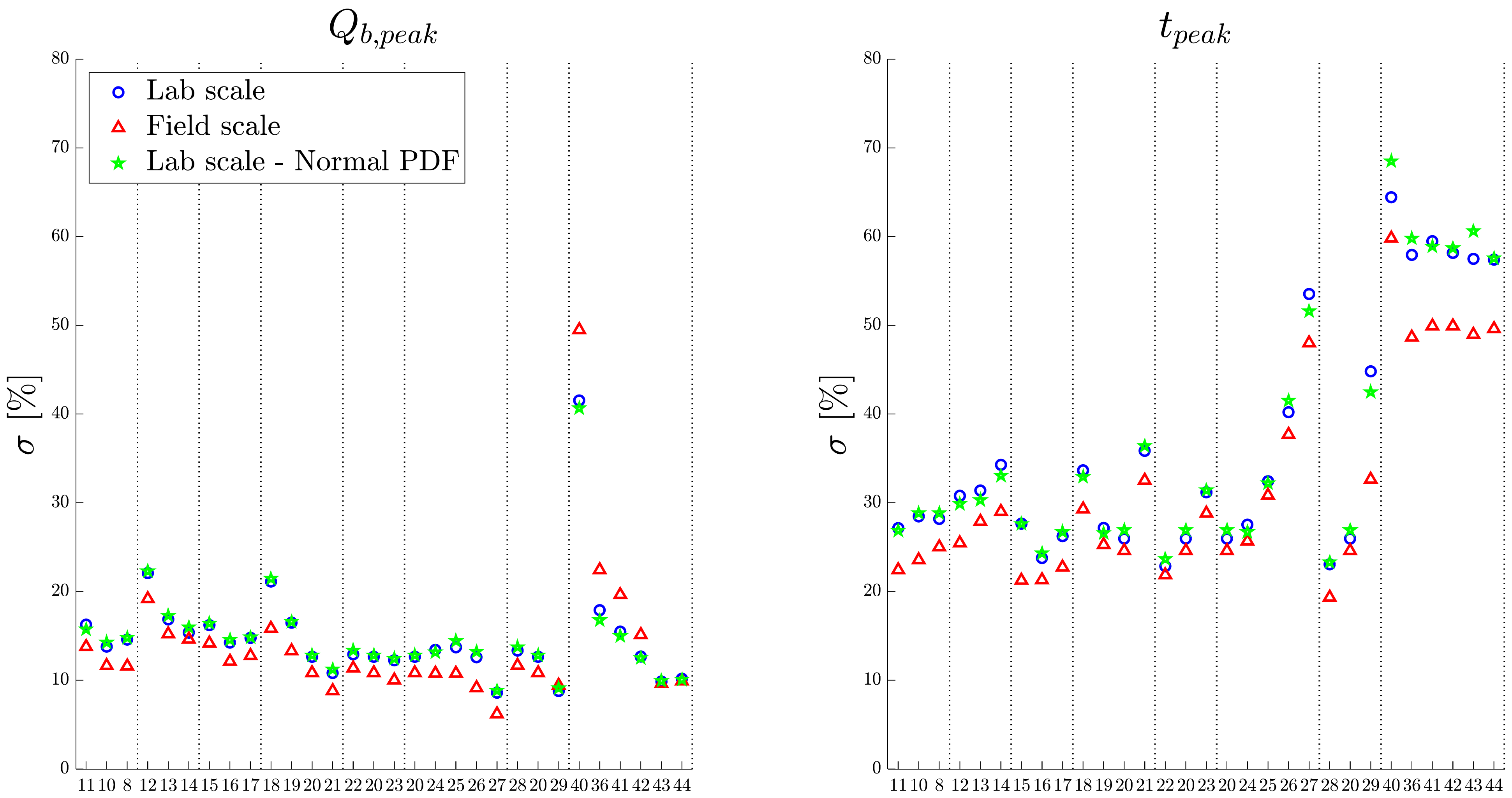

Figure S12 Standard deviation of the normalized and centred results = std(*output*/median(*output*) - 1). Green markers correspond to laboratory-scale configurations with truncated normal distributions associated to parameters c_{eff}, A_n, Q_{in}, θ_{σ}, λ and h_d.

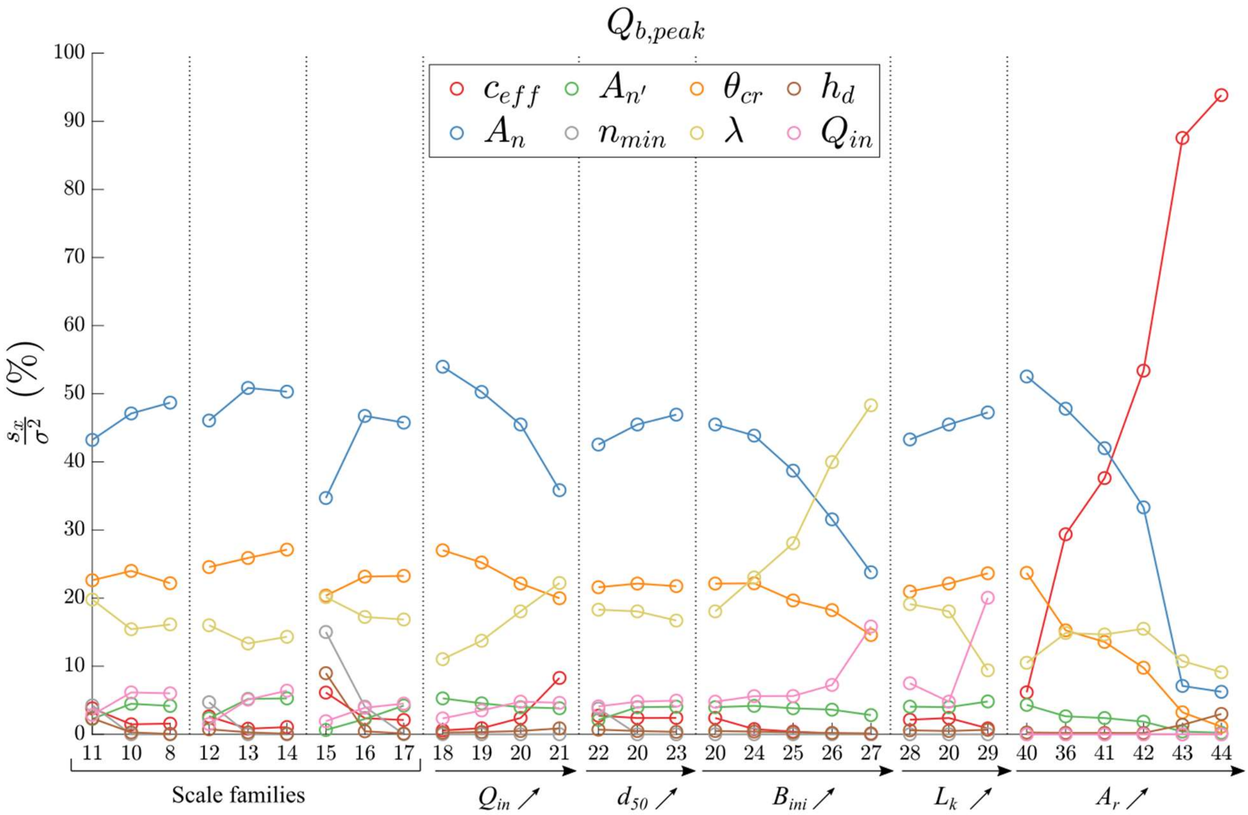

(a)

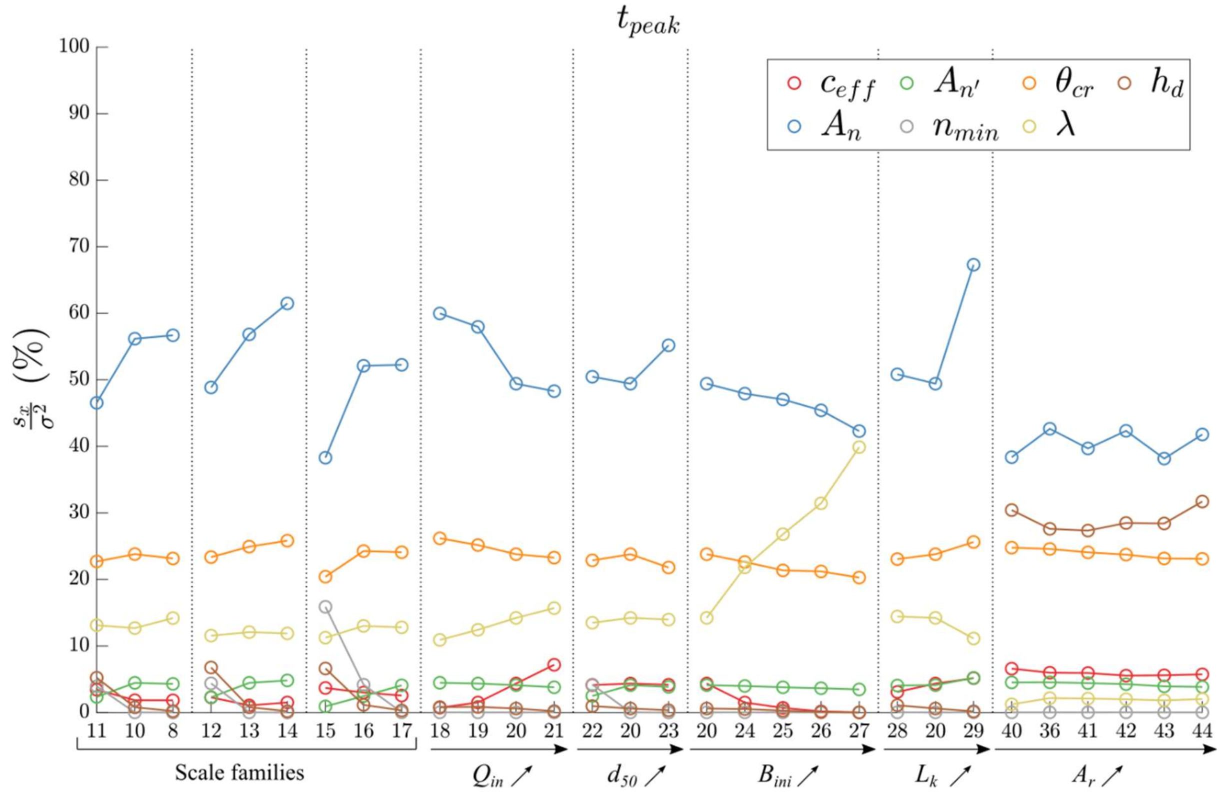

(b)

Figure S13 Sobol indices of total order for (a) peak breach discharge, and (b) time to peak in laboratory-scale configurations with truncated normal distributions associated to parameters c_{eff}, A_n, Q_{in}, θ_{cr}, λ and h_d.

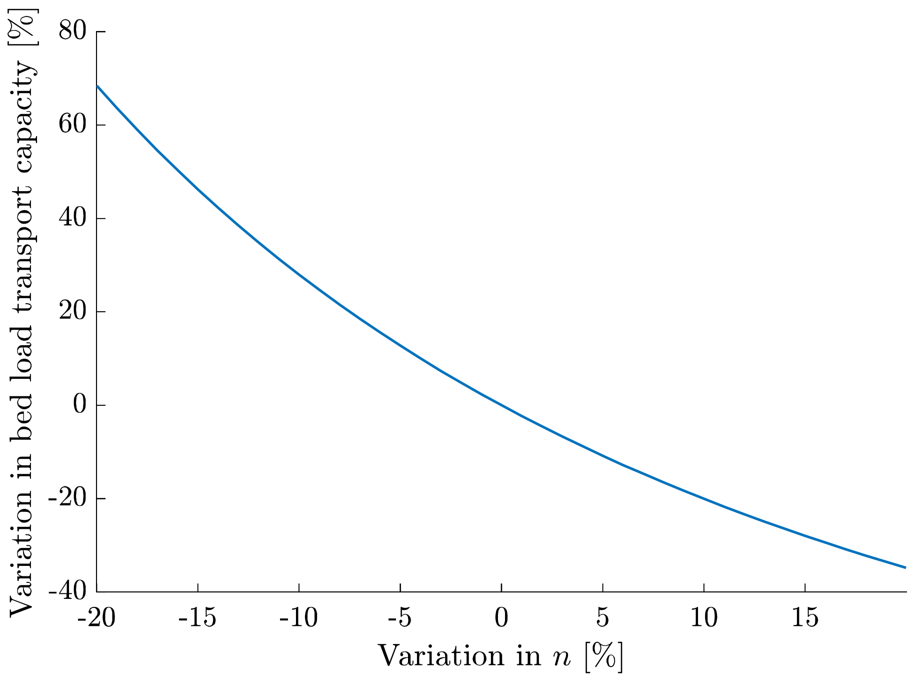

Figure S14 Variation in the bed load transport capacity as a function of a variation in the Manning's coefficient value in Test 10 at laboratory scale. The origin of the axes corresponds to the reference configuration of Test 10.